Open Veterinary Journal, (2023), Vol. 13(1): 64–73
ISSN: 2226-4485 (Print)
ISSN: 2218-6050 (Online)
Original Research
DOI: *10.5455/OVJ.2023.v13.i1.7*

Submitted: 14/06/2022 Accepted: 15/12/2022 Published: 12/01/2023

Clinicopathological study of sarcomatoid renal cell carcinoma in animals in East Java, Indonesia, from 2017 to 2022

Yos Adi Prakoso[1], Sitarina Widyarini[2*], Fradika Cahya Faresy[3] and Yudha Sapto Utomo[3,4]

[1]*Department of Pharmacology, Faculty of Veterinary Medicine, University of Wijaya Kusuma Surabaya, Surabaya, Indonesia*
[2]*Department of Pathology, Faculty of Veterinary Medicine, Universitas Gadjah Mada, Yogyakarta, Indonesia*
[3]*Master Program in Veterinary Science, Faculty of Veterinary Medicine, Universitas Gadjah Mada, Yogyakarta, Indonesia*
[4]*Master Program in Vaccinology and Immunotherapeutic, Faculty of Veterinary Medicine, University of Airlangga, Surabaya, Indonesia*

Abstract

Background: Renal cell carcinoma (RCC) is common cancer derived from the renal epithelium. One of the rarest cases of RCC is sarcomatoid RCC (sRCC). The occurrence of sRCC in animals is not clearly demonstrated.

Aim: This study aimed to observe the clinicopathological characteristics of sRCC in animals from East Java, Indonesia, from 2017 to 2022.

Methods: This study used patients who were histopathologically diagnosed with sRCC in our laboratory from 2017 to 2022. The data on the clinical characteristics of animals, hematology, serology, histopathology, and immunohistochemistry (IHC) were retrieved and tabulated. The data were qualitatively and quantitatively analyzed using a simple descriptive method and Statistical Package for the Social Sciences version 26, respectively.

Results: Fourteen cases of sRCC in animals have been identified in this study. It was found in rodents, dogs, and cats. sRCC predominantly occurred in rodents (57.14%) without specific clinical signs. The common histopathological findings of sRCC were epithelial renal cells transition into elongated atypical spindle cells. In addition, other histopathological patterns of a renal epithelial cell such as clear cell, tubule-cystic, and papillary also have been found. IHC by using antibodies demonstrates that PAX8 is expressed on sRCC tissue samples 92.85% (13/14 samples). Hence, PAX8 could be used as a supporting method for establishing the diagnosis of sRCC in animals. Hematology and serological tests did not correlate to the type of sRCC either pure sRCC or dedifferentiated sRCC. sRCC results in hypercreatinemia in rodents and dogs.

Conclusion: This study shows that the incidence of sRCC in animals is rare. Animals with sRCC did not show any specific clinical signs. The histopathological finding is quite difficult to be differentiated from the other RCC. PAX8 expression on renal tissue samples is useful in supporting the diagnosis of sRCC in animals.

Keywords: Animal, Kidney, PAX8, Renal cell carcinoma, Sarcomatoid.

Introduction

Renal cell carcinoma (RCC) is common cancer worldwide that differentiates from epithelial cells of the nephron (Hsieh *et al.*, 2017). In human medicine, the RCC is categorized into several tumor types including clear cell RCC (ccRCC), papillary RCC (PRCC), chromophobe RCC (chRCC), collecting duct carcinoma, tubulocystic RCC, MiT family translocation RCC, hereditary tumor, other tumor types, and unclassified RCC (Muglia and Prando, 2015). The unclassified RCC is the rarest case of RCC. Furthermore, the unclassified RCC is purely sarcomatoid and it belongs to sarcomatoid RCC (sRCC). The sRCC is an aggressive subtype of RCC presenting unusual morphological features with a poor prognosis (Yu *et al.*, 2017).

Unfortunately, there is no definite standard regarding the histopathological grading of RCC in veterinary medicine except for feline and canine RCC (Edmondson *et al.*, 2015). Veterinary pathologist commonly uses guideline from the human standard. Those problems impact the late diagnosis of this disease's pathogenesis. The tumor often reaches a bigger size before the occurrence of clinical signs. Lethargy, polydipsia, anorexia, cachexia, abdominal pain, and hematuria are the most common clinical signs in the incidence of sRCC (Gray and Harris, 2019).

***Corresponding Author:** Sitarina Widyarini. Department of Pathology, Faculty of Veterinary Medicine, Universitas Gadjah Mada, Yogyakarta, Indonesia. Email: *w.sitarina@gmail.com*

The sRCC is histopathologically characterized by spindle cells, fibrosarcoma, histiocytoma, chondrosarcoma, and others (Zhang *et al.*, 2019). Its unique morphological features trigger human medicine to use immunohistochemistry (IHC) to predict the transformation and determine the origin of renal sarcomatoid cells. Several eminent markers for sRCC in humans include CAIX, p53, bcl-2, CD10, PAX8, and CK7 (Blum *et al.*, 2020). It is suspected that those markers can be applied in veterinary medicine too. However, the scarce incidence of sRCC in animals makes little availability of clinicopathological data. Therefore, this study aimed to examine the clinicopathological characteristics of sRCC in animals from January 2017 until January 2022 in East Java, Indonesia.

Material and Methods

Samples

Fourteen animals that were histopathologically diagnosed with sRCC in the Integrated Laboratory, University of Muhammadiyah Sidoarjo, East Java from January 2017 until January 2022, were included in this study. All the reference samples were obtained from the veterinary clinics and laboratory of animal models in East Java. The data of animal species, gender, age, status, hematology, and serum profile were collected.

Blood and serum test

The blood was tested using an automated hematology analyzer (Medonic M-32 Series, MRK Diagnostics, Indonesia) against several parameters including red blood cells index, white blood cells (WBC), differential count, a total of platelets, and total protein plasma (TPP). The test was conducted following the manufacturing procedure. The serum samples were tested against liver and kidney function using several parameters including aspartate aminotransferase (AST), alanine aminotransferase (ALT), and blood urea nitrogen (BUN), and creatinine (CREAT). The AST/ALT was measured using the demonstrated procedure in a previous study (Kim *et al.*, 2020), as well as the measurement of BUN/CREAT (Uchino *et al.*, 2006).

Histopathology and IHC

The kidney tissue from the animals was collected by several procedures such as surgery, necropsy, and biopsy. The detail of the tissue collection procedure can be seen in Table 1. The kidney was soaked inside 10% neutral buffer formalin. After 24 hours, the samples were dehydrated using graded alcohol and xylene. The samples were embedded and blocked using liquid paraffin. The blocked tissues were sectioned using microtome in 0.3–0.5 µm of thickness and attached to the object-glass. Furthermore, the samples were stained using hematoxylin and eosin (H&E) and IHC.

The H&E staining was performed as routine staining. First, the slide was soaked using xylene and graded alcohol. The slide was then rinsed using tap water. The slide was soaked using hematoxylin, tap water, and eosin. At last, the slide was soaked using graded alcohol, and xylene, and mounted using Entellan.

Table 1. Clinical characteristic of the selected animals.

Patient code	Animal species	Sex	Age (Y, Mt)	Side	Size (cm)	SCT	Status	HD
R-1	Roborovski dwarf hamster	M	1,6	L	1.3	Surgery	DAS	+
R-2	Campbell hamster	M	0,8	R	0.5	Necropsy	DBS	+
R-3	Mouse-1	M	0,3	L	0.5	Necropsy	DBE	+
R-4	Mouse-2	F	0,6	L	1.0	Necropsy	DBE	+
R-5	Mouse-3	M	-	R	−	Necropsy	DBE	+
R-6	Sprague Dawley rat-1	M	0,7	R	−	Surgery	AAS	+
R-7	Sprague Dawley rat-2	F	0,3	R	−	Necropsy	DOC	−
R-8	Sprague Dawley rat-3	M	0,7	L	1.5	Necropsy	DBE	+
C-9	Mongrel-1	M	2,1	L	−	Biopsy	AAS	+
C-10	Mongrel-2	M	2,0	L	6.0	Biopsy	AAS	+
C-11	Mongrel-3	M	−	−	−	Necropsy	DOC	−
C-12	Pomeranian dog	F	1,8	R	8.0	Biopsy	AAS	+
F-13	Domestic cat-1	M	−	−	−	Necropsy	DOC	−
F-14	Domestic cat-2	M	−	−	−	Necropsy	DOC	−

(−): no available data; (+): available; (AAS): alive after surgery; (DAS): died after surgery; (DBE): died by euthanasia; (DBS): died before surgery; (DOC): died of unknown causes; (F): female; (HD): hematology data; (L): left; (M): male; (Mt): month; (R): right; (SCT): sample collection technique; (Y): year.

For IHC, the slide was deparaffinized and rehydrated using xylene and alcohol. The slide was retrieved using antigen retrieval solution (RE7113-CE, Leica Biosystem) and applied using the primary antibody against PAX8 (sc-81353, Santa Cruz, CA) and CK7 (sc-23976, Santa Cruz, CA). Further, the slides were processed following a previous study (Prakoso *et al.*, 2020). The slides were retrieved using an antigen retrieval solution at 98°C for 20 minutes. The slides were then incubated using peroxidase block and protein block. After that, they were incubated using a primary antibody (antibody anti-PAX8 and CK7), post-primary antibody, chromogen, and counter-stain. The slides were covered using Entellan and cover slip. The staining result was then analyzed using a light microscope (CX-33 Series, Olympus, Japan).

Morphometry

The morphometry of H&E slides was analyzed by a senior pathologist. The mitotic count was measured and standardized using the Fuhrman grading system (Edmondson *et al.*, 2015). The Fuhrman grading system was based on the nuclear and nucleolar morphology with four grades from grades I, II, III, and IV. In contrast, the IHC was analyzed and measured using a simple scoring system. The area that showed the immune expression of PAX8 and CK7 was scored as: 1 (immune-expressed) and 2 (no immune-expressed) (Palgunadi *et al.*, 2019).

Analysis data

The data of hematology were qualitatively analyzed and the interpretation of each hematological parameter was reported as a percentage. The data of histopathology were reported qualitatively and the immunohistochemical score was reported as the percentage. Further, the correlation between each parameter was analyzed using Fisher's exact test (Kim, 2017). All the statistical analysis was performed using Statistical Package for the Social Sciences version 26 with a p-value = 0.05.

Ethical approval

The ethical clearance committee from the Faculty of Dentistry, University of Airlangga, Surabaya has approved this study with registration number: 226/HRECC/FODM/IV/2020. All the samples were collected under the supervision of the veterinary clinician and veterinary pathologist. In addition, the owners' informed consent was received before the specimens were collected from pets.

Results

Clinical characteristics of animals

The sRCC predominantly occurred in rodents (eight cases), dogs (four cases), and cats (two cases). The rodents that suffered from sRCC were experimental rodents 75% and pet rodents (12.5% of Roborovski dwarf hamsters and 12.5% of Campbell hamsters). The experimental rodents were not showed any clinical signs; however, it was identified after the kidney tissue was diagnosed by the pathologist. In contrast, the pet rodents showed hematuria and anorexia. One of the pet rodents died before the surgery and the other one died after surgery. Unfortunately, there are only minimal data regarding the occurrence of sRCC in either canines or felines. During the past 5 years, there are only four cases of sRCC in dogs and two cases in cats (Table 1).

Hematology and serology

Based on the hematological test, various hematology changes are being observed including anemia, thrombocytosis, thrombocytopenia, hyperproteinemia, leukopenia, lymphocytosis, monocytosis, neutrophilia, uremia, hypercreatinemia, elevated AST and ALT (Table 2). Unfortunately, the hematological data were

Table 2. Hematological result of the selected animals.

Parameter	Number (%)		
	Rodent	Dog	Cat
Anemia	6 (85.71%)	1 (33.33%)	–
Thrombocytosis	1 (14.28%)	1 (33.33%)	–
Thrombocytopenia	1 (14.28%)	0 (0%)	–
Hyperproteinemia	3 (42.85%)	2 (66.66%)	–
Leukopenia	0 (0%)	1 (33.33%)	–
Lymphocytosis	1 (14.28%)	0 (0%)	–
Monocytosis	3 (42.85%)	2 (66.66%)	–
Neutrophilia	3 (42.85%)	1 (33.33%)	–
Uremia	4 (57.14%)	2 (66.66%)	–
Hypercreatinemia	7 (100%)	3 (100%)	–
Elevated AST	0 (0%)	1 (33.33%)	–
Elevated ALT	1 (14.28%)	0 (0%)	–

(–): no available data.

only available in 10 animals (7 rodents and 3 dogs) from a total of 14 animals (Table 1). The detail of the hematological result was shown in Table 2.

Histopathology

The tumor predominantly showed solid architecture in all collected animals. The sRCC was characterized by the gradual transition of the epithelial cells into elongated atypical spindle cells. Based on its appearance, we determined it as a pure sRCC. In contrast, there are several slides of sRCC that also showed the other patterns that are similar to the other type of RCC have been categorized as mixed sRCC or dedifferentiated sRCC. From a total of 14 specimens, there are 2/14 have been categorized as grade II, 9/14 (grade III), and 3/14 (grade IV). The other patterns include clear cells, tubule-cystic, and papillary patterns (Table 3).

Furthermore, the histopathological appearance of sRCC in rodents demonstrated the dual morphology either, normal or neoplastic depending on the grade of the tumor. Some of them showed that the neoplastic tissue depressed the normal tissue from the center to the edge (Fig. 1a). The abnormal mitotic figure (Fig. 1a), fibrous histiocytoma-like cells (Fig. 1b), emperipolesis (Fig. 1c), and osseous metaplasia (Fig. 1d) have been identified in rodents. Moreover, the cystic and papillary architecture was also observed in the dogs' kidneys (Fig. 2a–c). In cats, the sRCC presented osseous metaplasia with glomeruloid bodies (Fig. 3a and b) and eosinophilic cytoplasm with psammoma bodies (Fig. 3c and d).

Immunohistochemistry

This study used two types of IHC markers including PAX8 and CK7. Those two IHC markers represented various results regarding their positivity and negativity immune reactions. From a total of 14 samples, as many as 13 (92.85%) samples were positive against PAX8 except for one sample from the SD rat-3. In contrast, the expression of CK7 was only detected in 3/14 (21.42%) samples. Those samples were Roborovski dwarf hamster, SD rat-2, and Pomeranian dog (Table 4).

Correlation between parameters

The result showed that there is no correlation between the type of sRCC (pure and dedifferentiated) with the species of animals with $p = 0.30$ ($p \geq 0.05$). It indicated that the occurrence of the sRCC is not dependent on the animal species. Further, the type of sRCC does not correlate with the sex, hematology, and serology of the collected samples (Table 5). The immune expression of PAX8 that consistently expressed on the tumor tissue however, it has no correlation with the type of sRCC as well as CK7 (Table 6).

Discussion

The incidence of sRCC in animals is relatively rare and similar to the incidence of this disease in humans. The sRCC is spontaneously occurring in animals with no understanding of the disease etiology. This study shows that the most frequent cases occur in rodents especially, experimental rodents (6/8). The anamnesis showed that most experimental rodent samples were collected during euthanasia (66.66%) and accidentally

Table 3. Histopathology finding of sRCC in the selected animals.

Patient code	Grade	APt	SPt	PB	PPt	OM	CCPt	CyPt	GB
R-1	III	+	+	+	−	−	−	−	−
R-2	IV	+	+	−	−	−	−	−	−
R-3	III	+	+	−	+	−	−	−	−
R-4	III	+	+	−	+	−	−	+	+
R-5	III	+	+	−	+	−	−	−	+
R-6	III	+	+	+	−	+	−	−	−
R-7	II	+	+	+	−	+	+	−	−
R-8	IV	+	+	−	−	−	+	−	+
C-9	IV	+	+	+	+	−	+	+	−
C-10	III	+	+	+	+	−	−	+	−
C-11	III	+	+	−	+	−	+	+	+
C-12	II	+	+	+	+	−	+	+	−
F-13	III	+	+	+	+	+	−	−	+
F-14	III	+	+	+	−	+	−	−	+

(−): not observed; (+): observed; (Apt): atypical pattern; (CCPt): clear cell pattern; (CyPt): cyctic pattern; (GB): glomeruloid bodies; (OM): osseous metaplasia; (PB): Psammoma bodies; (PPt): papillary pattern; (SPt): spindloid pattern.

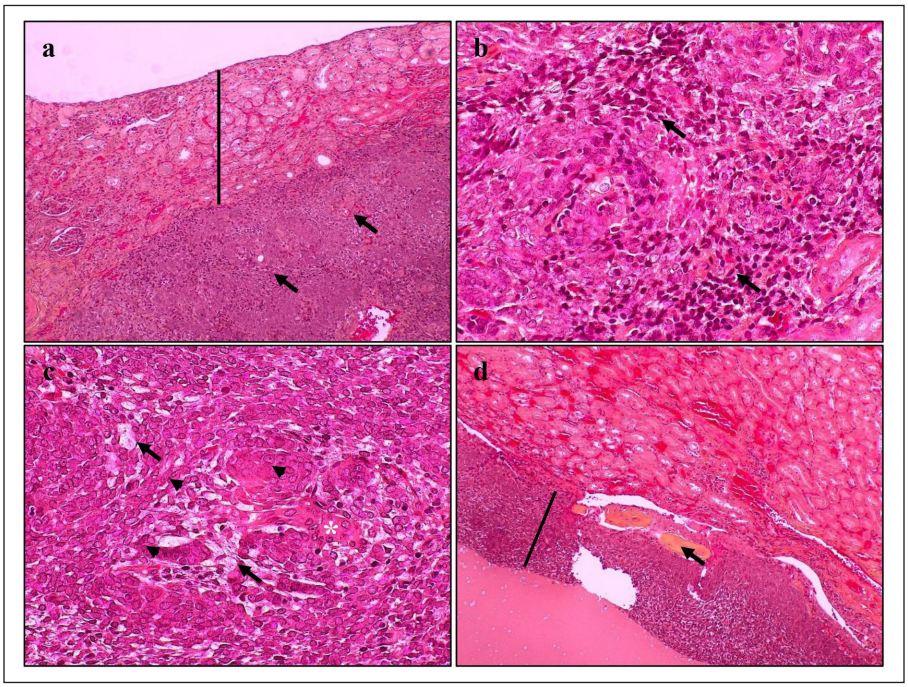

Fig. 1. Histopathology of sRCC in rodents. Tumor mass of a kidney of hamster-1 showed dual morphology with abnormal mitotic figures (arrow) and the normal tissue (line) was depressed to the edge (a); fibrous histiocytoma-like cells (arrow) with nuclear pleomorphism in the kidney of hamster-2 (b); the kidney of mouse-2 represent clear cell carcinoma (arrow) surrounded by atypical spindle cells (arrowhead) with eosinophilic cytoplasm and emperipolesis (asterisks) (c); high vascularization with osseous metaplasia (arrow) surrounded by abnormal mitotic architecture (line) in the kidney of SD rat-2 (d). H and E, 100× (a, d), 400× (b, c).

diagnosed as sRCC. It is similar to the occurrence of sRCC in cats in this study. Only one sample from the dog (Pomeranian dog) showed clinical signs such as hematuria and anorexia. This study proves that the animals can be suffering from sRCC without specific clinical signs and commonly they were diagnosed after the sample was collected.

The difficulty in diagnosing sRCC was aggravated by unspecific clinical signs and the result of the hematological test, either. The most common hematological results that occur concomitantly with sRCC in this study were anemia, uremia, and hypercreatinemia (Table 2). Anemia occurs during sRCC due to the massive disruption of iron homeostasis (Portolés *et al.*, 2021). During the RCC, the iron is deposited within the extracellular space because the kidney failed to filter and reabsorbed iron as a source of erythropoietin and hemoglobin synthesis. The mechanism of iron deposit has been confirmed in promoting tumor growth (Schnetz *et al.*, 2020). The tumor progression in sRCC can cause the elevate of circulating toxins such as urea nitrogen and CREAT that refer to as azotemia (Akcay *et al.*, 2010). Physiologically, urea nitrogen is a product of protein metabolism and can be used as a heart failure biomarker. And CREAT itself is a nonprotein nitrogenous substance that is produced by the catabolism of phosphocreatine. The CREAT can be filtered in glomeruli and excreted in conjunction with the urine (Hurabielle *et al.*, 2016). The accumulation both of urea nitrogen and CREAT within the blood indicates the decrease of glomerular filtration rate as the compensatory impact of changes in the structure and function of glomeruli and tubule within the kidney parenchyma.

The sRCC is marked by the metastasis of the epithelial cells of renal tubules from cuboidal cells into elongated atypical spindle cells (Moch *et al.*, 2016). The mitotic index is a major indicator in presenting the reports of this disease. During the last 5 years, only 14 animals are suffering from sRCC and there are only 4 animals (3 rodents and 1 cat) that showed pure sRCC. In contrast, the rest of them shows the sarcomatoid type that is accompanied by the other architectures (dedifferentiated type) including papillary, clear cell, and cystic pattern. Furthermore, osseous metaplasia with glomeruloid bodies has been observed in several specimens. Osseous metaplasia is the common metaplastic transformation within a soft tissue such as the endometrial tissue (Prakoso *et al.*, 2019), however, the presentation of osseous metaplasia within the

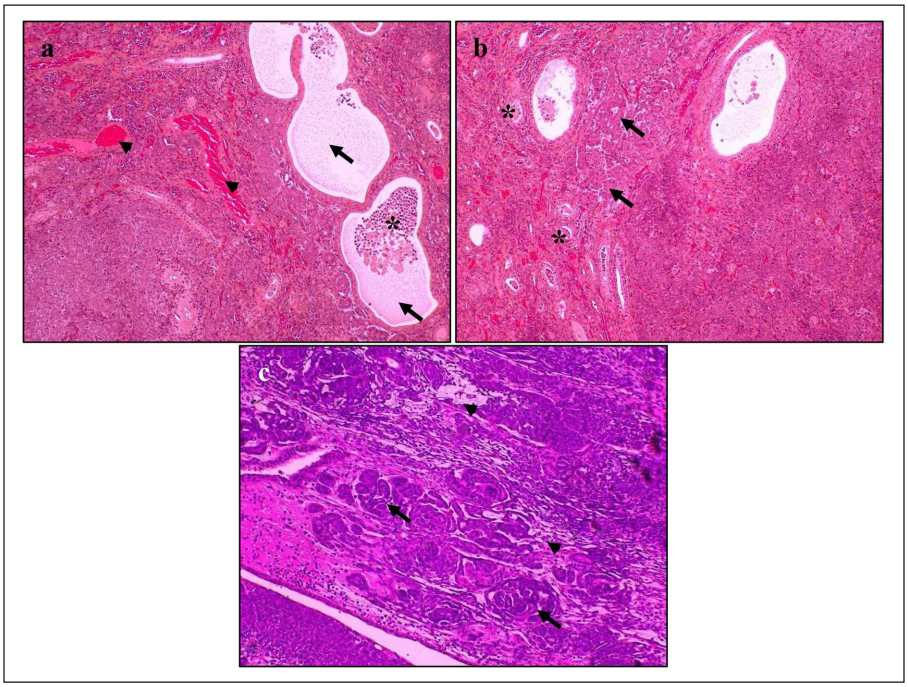

Fig. 2. Histopathology of sRCC in dogs. The kidney of mongrel-2 showed renal cystic (arrow) in the center of tumor mass, the cell debris (asterisks) was found inside the lumen, high vasculature (arrowhead), and dual morphology was observed (a); the tumor of the kidney in mongrel-3 showed papillary architecture (arrow) with high grade of nuclei and psammoma bodies (asterisks) (b); the sarcomatoid with papillary structures (arrow) and clear cell carcinomas (arrowhead) were observed in the tumor mass of kidney from Pomeranian dog (c). H and E, 100× (a–c).

kidney is a rare and unique case. The other findings are the fibrous histiocytoma-like cells and emperipolesis. Fibrous histiocytoma-like cells occur with nuclear polymorphism as an indication that there is a mitosis of mesenchymal cells. The tumor invasion within the normal tissue conducts active penetration to an intact tissue and generates emperipolesis (Rastogi *et al.*, 2014). During the tumor invasion, the proliferation of microvascular is an eminent risk factor. The glomeruloid bodies are a unique form of microvascular resembling abortive papillae (Döme *et al.*, 2003). It represents the lymphocyte infiltration-like within the lumen shrouded by pseudocapsule. The proliferation of glomeruloid bodies is commonly accompanied by the appearance of psammoma bodies. Interestingly, another histopathological pattern that belongs to other RCC types has been observed.

The occurrence of another type of RCC in conjunction with the sRCC is caused by a variety of renal epithelial cells. The variety of nephrons possibly contributes to the distinct neoplastic condition either pure sRCC or dedifferentiated sRCC. The previous study described that the sRCC commonly appears as a complex tumor mass and could be found to grow together with the other RCC (Pichler *et al.*, 2019). Nevertheless, a clear mechanism regarding the dedifferentiation of sarcomatoid types is unclearly understood. The transcription factor is suspected to contribute to tumorigeneses, such as Snail, Twist, and Zeb. The transcription factor increased the epithelial-mesenchymal transition process (Capasso *et al.*, 2020).

PAX8 is a potential transcription marker during kidney development. However, it also has a role in tumor development (Li *et al.*, 2011). PAX8 is a useful marker to distinguish the malignancies of the tumor specimens. This study indicates that sRCC also presents the expression of PAX8 (92.85%). In contrast, the previous study described that PAX8 is strongly expressed in RCC especially clear cell carcinoma (80.95%), however, it is less expressed in the sarcomatoid type (26.19%) (Yu *et al.*, 2017). The other study reported that it can be expressed on 100% of specimens in ccRCC (Mentrikoski *et al.*, 2014). These differences are due to the tumor differentiation level. The PAX8 is extensively expressed within the high-differentiated areas of the tumor. The other factors that may contribute are the utilization of different types and brands of primary antibodies based on their sensitivity and specificity.

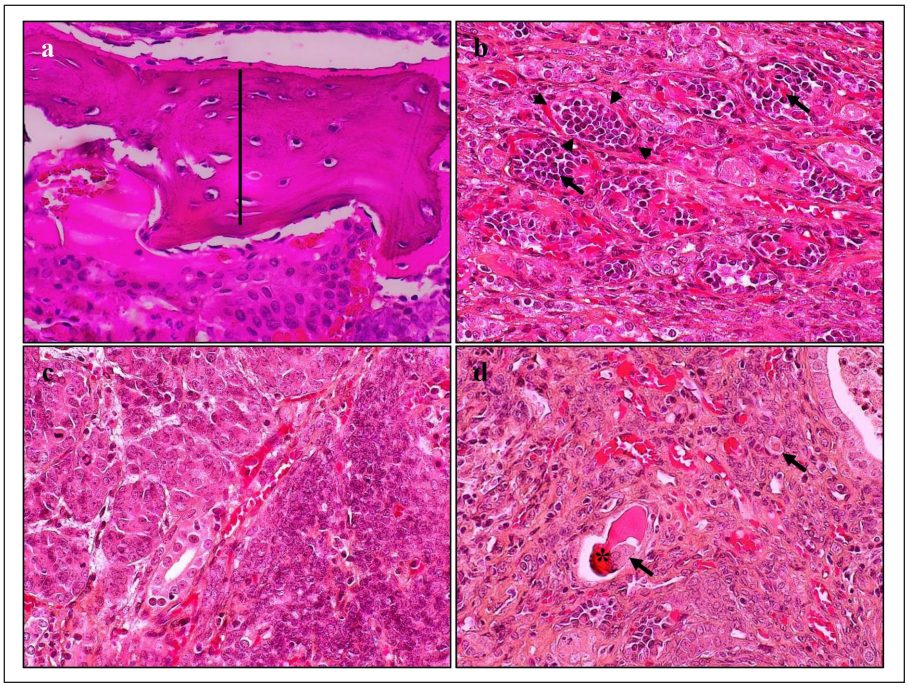

Fig. 3. Histopathology of sRCC in cats. The domestic cat-1 kidney showed osseous metaplasia (line) in the center of tumor mass (a); and the other corner presented glomeruloid bodies (arrow) shrouded by pseudocapsule (arrowhead) (b); atypical spindle cells with eosinophilic cytoplasm (c); psammoma body (asterisks), and foamy macrophages (arrow) were observed from the kidney of domestic cat-2 (d). H and E, 400× (a–d).

Table 4. IHC of PAX8 and CK7 of sRCC in the selected animals.

Parameter	Number (%)	
	PAX8	CK7
Rodent	7/14 (50.00%)	2/14 (14.28%)
Dog	4/14 (28.57%)	1/14 (7.14%)
Cat	2/14 (14.28%)	0/14 (0%)
Total	13/14 (92.85%)	3/14 (21.42%)

Unfortunately, the systemic evaluation of PAX8 during metastasis is not well explored. The advanced evaluation that includes the complex mechanism of PAX8 should be identified to generate a more accurate diagnostic tool for sRCC in animals.

In contrast, there is a minimal expression of CK7 compared to the PAX8. Less expression of CK7 (21.42%) indicated that this marker was not consistently expressed during the pathogenesis of sRCC. It is also explained the low sensitivity of this marker in sRCC. A previous study by Gonzalez *et al.* (2019) described that CK7 was highly expressed during the occurrence of clear cell carcinomas. Furthermore, the staining extends to CK7 depending on the grade of the tumor. Another report described that CK7 immune expression was found in RCC (ccRCC, PRCC, and chRCC) rather than the others (Ma *et al.*, 2016).

Further analysis analyzed the correlation between several eminent factors that may be contributing to the incidence of sRCC either pure or dedifferentiated. Unfortunately, there is no correlation between the potential parameters (animal species, sex, hematological profile, kidney and liver function, and even PAX8 and CK7) with the type of sRCC. There is no correlation between each factor and the type of sRCC in this study was suspected caused by the limited number of samples. The limited data cause bias during the data analysis and interpretation. The small data maybe catch the attention of precision; however, the large datasets may help in reducing bias. However, if the data have low reliability, they will be only focused on the random variation (Kaplan *et al.*, 2014). This study only used 14 data from 14 animals during the last past 5 years. The limited data in this study were caused by the minimum number of clinical cases. It proved that the incidence of sRCC in animals occurs spontaneously with unspecific clinical signs. However, it is still possible to analyze larger datasets using a wide range of observation years. It can be concluded that during the last 5 years, we found that the incidence of sRCC in animals is a rare disease. The animals suffering from sRCC are not showing specific clinical signs. Furthermore,

Table 5. Correlation between type of sRCC and hematology parameters in this study.

Parameters	Indicators	Type of sRCC		*p*-value
		Pure sRCC	Dedifferentiated sRCC	
Species of animal	Rodent	3	5	0.30
	Dog	0	4	
	Cat	1	1	
Sex	Male	4	7	0.50
	Female	0	3	
Anemia	ANN	2	2	0.36
	ANH	1	0	
	AMN	0	1	
	AMaN	0	1	
TPP	Hyperproteinemia	1	3	0.94
	Normal	2	4	
	Hypoproteinemia	0	0	
Thrombocyte	Thrombocytosis	0	2	0.58
	Normal	3	4	
	Thrombocytopenia	0	1	
WBC	Leukocytosis	0	1	0.76
	Normal	3	6	
	Leukopenia	0	0	
Monocyte	Monocytosis	2	2	0.51
	Normal	1	5	
	Monocytopenia	0	0	
Neutrophil	Neutrophilia	2	2	0.51
	Normal	0	0	
	Neutropenia	1	5	
BUN	Elevated	2	4	0.77
	Normal	1	3	
	Lower	0	0	
CREAT	Elevated	3	7	0.85
	Normal	0	0	
	Lower	0	0	
AST	Elevated	0	1	0.76
	Normal	3	6	
	Lower	0	0	
ALT	Elevated	1	0	0.25
	Normal	2	7	
	Lower	0	0	

the hematology and serological tests cannot support identifying the pathogenesis of sRCC in this study. The histopathological finding is quite difficult to be differentiated from the other RCC due to the overlapping architecture that is similar to the other type of RCC (dedifferentiated). This study demonstrated that PAX8 can be useful in supporting the diagnosis of sRCC in animals, however, larger datasets must be

Table 6. Correlation between type of sRCC and the immune expression of PAX8 and CK7.

Parameters	Indicators	Type of sRCC		*p*-value
		Pure sRCC	Dedifferentiated sRCC	
PAX8	Positive	4	9	1.000
	Negative	0	1	
CK7	Positive	1	2	1.000
	Negative	3	8	

collected to increase the specificity and sensitivity of this IHC marker.

Acknowledgments

The authors would like to thank all pathologists and veterinary technicians from the Laboratory of Pathology, Disease Investigation Center of Wates, Yogyakarta, who support to give some second opinions during this study.

Conflict of interest

The authors declare that they have no conflict of interest.

Author contributions

YAP, SW, FCF, and YSU were responsible for collecting the specimens. YAP and SW analyzed the histopathological specimens. FCF and YSU performed the laboratory analysis of the hematological data. All the authors were involved in the data interpretation, writing the draft of the manuscript, revising, and giving final approval for the submitted and published manuscript.

References

Akcay, A., Turkmen, K., Lee, D. and Edelstein, C.L. 2010. Update on the diagnosis and management of acute kidney injury. Int. J. Nephrol. Renovasc. Dis. 3, 129–140.

Blum, K.A., Gupta, S., Tickoo, S.K., Chan, T.A., Russo, P., Motzer, R.J., Karam, J.A. and Hakimi, A.A. 2020. Sarcomatoid renal cell carcinoma: biology, natural history and management. Nat. Rev. Urol. 17(12), 659–678.

Capasso, M., Lasorsa, V.A., Cimmino, F., Avitabile, M., Cantalupo, S., Montella, A., De Angelis, B., Morini, M., de Torres, C., Castellano, A., Locatelli, F. and Iolascon, A. 2020. Transcription factors involved in tumorigenesis are over-represented in mutated active DNA-binding sites in neuroblastoma. Can. Res. 80(3), 382–393.

Döme, B., Tímár, J. and Paku, S. 2003. A novel concept of glomeruloid body formation in experimental cerebral metastases. J. Neuro. Exp. Neuron. 62(6), 655–661.

Edmondson, E.F., Hess, A.M. and Powers, B.E. 2015. Prognostic significance of histologic features in canine renal cell carcinomas: 70 nephrectomies. Vet. Pathol. 52(2), 260–268.

Gonzalez, M.L., Alaghehbandan, R., Pivovarcikova, K., Michalova, K., Rogala, J., Martinek, P., Foix, M.P., Mundo, E.C., Comperat, E., Ulamec, M., Hora, M., Michal, M. and Hes, O. 2019. Reactivity of CK7 across the spectrum of renal cell carcinomas with clear cells. Histopathology 74(4), 608–617.

Gray, R.E. and Harris, G.T. 2019. Renal cell carcinoma: diagnosis and management. Am. Fam. Physician. 99(3), 179–184.

Hsieh, J.J., Purdue, M.P., Signoretti, S., Swanton, C., Albiges, L., Schmidinger, M., Heng, D.Y., Larkin, J. and Ficarra, V. 2017. Renal cell carcinoma. Nat. Rev. Dis. Prim. 3, 17009.

Hurabielle, C., Pillebout, E., Stehlé, T., Pagès, C., Roux, J., Schneider, P., Chevret, S., Chaffaut, C., Boutten, A., Mourah, S., Basset-Seguin, N., Vidal-Petiot, E., Lebbé, C. and Flamant, M. 2016. Mechanisms underpinning increased plasma creatinine levels in patients receiving vemurafenib for advanced melanoma. PLoS One 11(3), e0149873.

Kaplan, R.M., Chambers, D.A. and Glasgow, R.E. 2014. Big data and large sample size: a cautionary note on the potential for bias. Clin. Transl. Sci. 7(4), 342–346.

Kim, H.J., Kim, S.Y., Shin, S.P., Yang, Y.J., Bang, C.S., Baik, G.H., Kim, D.J., Ham, Y.L., Choi, E.Y. and Suk, K.T. 2020. Immunological measurement of aspartate/alanine aminotransferase in predicting liver fibrosis and inflammation. Korean J. Intern. Med. 35(2), 320–330.

Kim, H.Y. 2017. Statistical notes for clinical researchers: chi-squared test and Fisher's exact test. Restor. Dent. Endod. 42(2), 152–155.

Li, C.G., Nyman, J.E., Braithwaite, A.W. and Eccles, M.R. 2011. PAX8 promotes tumor cell growth by transcriptionally regulating E2F1 and stabilizing RB protein. Oncogene 30(48), 4824–4834.

Ma, F., Dai, L., Wang, Z., Zhou, L., Niu, Y. and Jiang, N. 2016. Evaluating prognosis by CK7 differentiating renal cell carcinomas from oncocytomas can be used as a promising tool for optimizing diagnosis strategies. Oncotarget. 7(29), 46528–46535.

Mentrikoski, M.J., Wendroth, S.M. and Wick, M.R. 2014. Immunohistochemical distinction of renal cell carcinoma from other carcinomas with clear-cell histomorphology: utility of CD10 and CA-125 in addition to PAX-2, PAX-8, RCCma, and adipophilin. Appl. Immunohistochem. Mol. Morphol. 22(9), 635–641.

Moch, H., Cubilla, A.L., Humphrey, P.A., Reuter, V.E. and Ulbright, T.M. 2016. The 2016 WHO classification of tumours of the urinary system and male genital organs-part A: renal, penile, and testicular tumours. Eur. Urol. 70(1), 93–105.

Muglia, V.F. and Prando, A. 2015. Renal cell carcinoma: histological classification and correlation with imaging findings. Radiol. Bras. 48(3), 166–174.

Palgunadi, B.U., Kurniasih and Prakoso, Y.A. 2019. Risk factor of renal aspergillosis in pigeons (*Columba livia*): field study. Am. J. Anim. Vet. Sci. 14(2), 78–85.

Pichler, R., Compérat, E., Klatte, T., Pichler, M., Loidl, W., Lusuardi, L. and Schmidinger, M. 2019. Renal cell carcinoma with sarcomatoid features: finally new therapeutic hope? Cancers 11(3), 422.

Portolés, J., Martín, L., Broseta, J.J. and Cases, A. 2021. Anemia in chronic kidney disease: from pathophysiology and current treatments, to future agents. Front. Med. 8, 642296.

Prakoso, Y.A., Rini, C.S., Rahayu, A., Sigit, M. and Widhowati, D. 2020. Celery (*Apium graveolens*) as a potential antibacterial agent and its effect on cytokeratin-17 and other healing promoters in skin wounds infected with methicillin-resistant *Staphylococcus aureus*. Vet. World. 13(5), 865–871.

Prakoso, Y.A., Widyawati, R., Wirjaatmadja, R., Kurnianto, A., and Kurniasih. 2019. Mixed mammary carcinosarcoma in domesticated Asian palm civet (*Paradoxurus hermaphroditus*). World. Vet. J. 9(1), 46–51.

Rastogi, V., Sharma, R., Misra, S.R., Yadav, L. and Sharma, V. 2014. Emperipolesis—a review. J. Clin. Diagn. Res. 8(12), ZM01–ZM2.

Schnetz, M., Meier, J.K., Rehwald, C., Mertens, C., Urbschat, A., Tomat, E., Akam, E.A., Baer, P., Roos, F.C., Brüne, B. and Jung, M. 2020. The disturbed iron phenotype of tumor cells and macrophages in renal cell carcinoma influences tumor growth. Cancers. 12(3), 530.

Uchino, S., Bellomo, R., Goldsmith, D., Bates, S. and Ronco, C. 2006. An assessment of the RIFLE criteria for acute renal failure in hospitalized patients. Crit. Care Med. 34(7), 1913–1917.

Yu, W., Wang, Y., Jiang, Y., Zhang, W. and Li, Y. 2017. Distinct immunophenotypes and prognostic factors in renal cell carcinoma with sarcomatoid differentiation: a systematic study of 19 immunohistochemical markers in 42 cases. BMC Cancer 17(1), 293.

Zhang, H., Majeed, N.K., Sharifi, R. and Guzman, G. 2019. A case of sarcomatoid renal cell carcinoma with osseous metaplasia and papillary renal cell carcinoma metastasis. Clin. Pathol. 12, 2632010X19848005.